Soft x-ray magnetic circular dichroism study of the ferromagnetic spinel-type Cr chalcogenides

A. Kimura*

Synchrotron Radiation Laboratory, Institute for Solid State Physics, University of Tokyo, Roppongi, Minato-ku, Tokyo 106-8666, Japan

J. Matsuno, J. Okabayashi, and A. Fujimori

Department of Physics, University of Tokyo, Bunkyo-ku, Tokyo 113-0033, Japan
and Department of Complexing Science and Engineering, University of Tokyo, Bunkyo-ku, Tokyo 113-0033, Japan

T. Shishidou

Department of Quantum Matter, ADSM, Hiroshima University, 1-3-1 Kagamiyama, Higashi-Hiroshima 739-8526, Japan

E. Kulatov

General Physics Institute, Russian Academy of Sciences, Vavilov Street 38, Moscow 117942, Russia

T. Kanomata

Department of Applied Physics, Faculty of Engineering, Tohoku Gakuin University, Tagajo, Miyagi 985-8537, Japan

We have observed magnetic circular dichroism (MCD) in the soft x-ray absorption spectra of the semiconducting ferromagnet $CdCr_2Se_4$ and the metallic ferromagnets $CuCr_2S_4$ and $CuCr_2Se_4$. The Cr $2p$ x-ray absorption and MCD spectra show that the d-electron occupancies of the Cr atom in the Cu based Cr sulfide and selenide are not much different from that in the $CdCr_2Se_4$ in spite of the different formal valencies $Cr^{3.5+}$ and Cr^{3+}, respectively. The observed Cu $2p$ MCD spectra show the existence of small magnetic moments on the Cu sites which are aligned antiparallel to the Cr $3d$ moment in $CuCr_2S_4$ and $CuCr_2Se_4$, consistent with band-structure calculation.

I. INTRODUCTION

Among spinel-type transition-metal compounds $CdCr_2S_4$ and $CdCr_2Se_4$ are ferromagnetic semiconductors with Curie temperatures of 85 and 129.5 K, respectively, and have been extensively studied because of their unusual optical and magnetic properties.[1,2] Their electronic structures have been studied by band-structure calculations[3,4] and photoemission spectroscopy.[5,6] The band-structure calculations explain well the redshifts of the optical absorption at 1.85 eV for the sulfide and that at 1.1–1.3 eV in the selenide with decreasing temperature across the magnetic phase transition. Here, the absorption is assigned to a transition from the Cr $3d$ t_{2g} band to the conduction band. The calculated band structure is also qualitatively consistent with the resonant photoemission result,[6] which has revealed the Cr $3d$ $t_{2g}\uparrow$ states as well as the $e_g\uparrow\downarrow$ states hybridized into the Se $4p$ band.

$CuCr_2S_4$, $CuCr_2Se_4$, and $CuCr_2Te_4$, on the other hand, show metallic conductivity and order ferromagnetically below the Curie temperatures well above room temperature, i.e., $T_C=377$ K for $CuCr_2S_4$, $T_C=430$ K for $CuCr_2Se_4$, and $T_C=360$ K for $CuCr_2Te_4$. The metallic character and the magnetic moment of approximately $5\mu_B$ per formula unit for $CuCr_2X_4$ ($X=$ S, Se, Te) have promoted interest in these compounds as promising materials for magneto-optical devices. The magneto-optical Kerr effect measurements on $CuCr_2Se_4$ single crystals between 0.55 and 5.0 eV show that the Kerr ellipticity ϵ_K reaches $-1.19°$ at 0.96 eV. In contrast to the Cd-based Cr spinel compounds, the electronic structure of the Cu-based Cr spinels has been studied less exten-

sively. Lotgering *et al.*[7] have explained the properties of $CuCr_2X_4$ assuming the mixed-valence state of $Cr^{3+}(d^3)$ and $Cr^{4+}(d^2)$ and $Cu^+(d^{10})$. This explanation is based on the assumption that the diamagnetic Cu^+ ions occupy the tetrahedral sites and the ferromagnetic moment arises from the parallel alignment of the spins of Cr^{3+} and Cr^{4+} located at the octahedral sites. The metallic conduction and the ferromagnetism have been attributed to double exchange between Cr^{3+} and Cr^{4+}. Goodenough,[1] on the other hand, has proposed that the octahedral sites are occupied by the Cr^{3+} ions so that the tetrahedral sites are occupied by formally divalent Cu ions. Recently, giant magnetoresistance was reported for $Fe_{1-x}Cu_xCr_2S_4$, invoking renewed interest in this type of materals.[8] So far, the detailed electronic structure has not been investigated based on, for example, band-structure calculations instead of the simple ionic model.

Soft x-ray core-level absorption spectroscopy of ferromagnetic materials using circularly polarized synchrotron light is well known to produce magnetic circular dichroism (MCD), which is defined as the difference between the absorption coefficient excited by incident light of opposite helicities. It is also known that MCD signals provide us with a quantitative value for the orbital magnetic moment as well as the spin magnetic moment using sum rules.[9,10] In order to clarify the electronic states responsible for the ferromagnetism on each site of the Cr spinel chalcogenides, we have performed a soft x-ray core absorption spectroscopy study for the semiconducting ferromagnet $CdCr_2Se_4$ and the metallic Cu-based ferromagnets $CuCr_2S_4$ and $CuCr_2Se_4$ using circularly polarized synchrotron radiation. The resulting
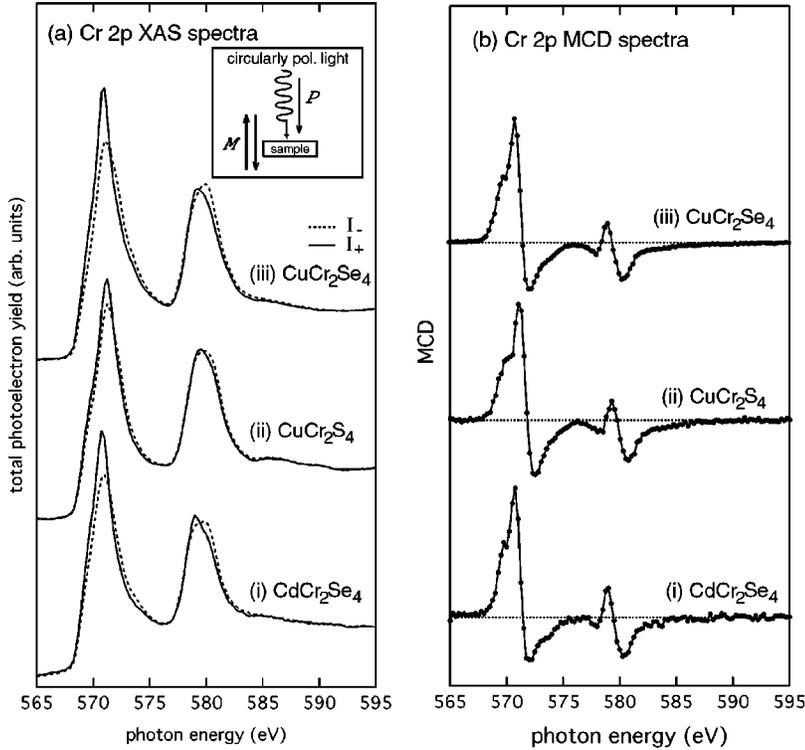
FIG. 1. Cr $2p$ (a) XAS and (b) MCD spectra of (i) $CdCr_2Se_4$, (ii) $CuCr_2S_4$, and (iii) $CuCr_2Se_4$. I_+ (I_-) is indicated by solid (dashed) line. The inset shows the experimental geometry for the light incidence and the magnetization of the sample (see text).

MCD signals inform us of the orbital and spin moments at different sites of the Cr spinel compounds. In addition, a relativistic linear-muffin-tin-orbital (LMTO) band-structure calculation has been carried out to interpret the MCD result within a one-electron approximation.

II. EXPERIMENTAL

Cr $2p$ and Cu $2p$ x-ray absorption spectroscopy (XAS) and MCD spectra were measured at beamline NE1B of the Accumulation Ring at High Energy Accelerator Research Organization (KEK). Circularly polarized light was supplied from a helical undulator, with which almost 100% polarization was obtained at the peak of the first-harmonic radiation. XAS spectra were measured by means of the total photoelectron yield by directly detecting the sample current with changing the photon energy $h\nu$. The photon energy resolutions were estimated to be 0.5 and 1 eV for Cr $2p$ and Cu $2p$ core absorption regions, which were determined from a gas phase measurement and a ray trace simulation of the beamline.[11] The meaurement was performed in the Faraday geometry, i.e., with both the incident light and the magnetization perpendicular to the sample surface as shown in the inset of Fig. 1. We used two pairs of Nd-Fe-B permanent dipole magnets with holes for passing the excitation light. The field of ~ 1.1 T at the sample position was alternatively reversed by setting one of the two dipole magnets on the optical axis by means of a moter-driven linear feedthrough.[12] The MCD spectra were taken for a fixed helicity of light by reversing the applied magnetic field at each $h\nu$. In the present paper, the MCD spectrum is defined as $I_+ - I_-$, where I_+ and I_- represent the absorption spectra for the direction of magnetization (which is opposite to the direction

of the majority spin) parallel and antiparallel to the photon spin (helicity), respectively. Clean surfaces were obtained by *in situ* scraping of the samples with a diamond file in ultra-high vacuum condition. The cleanliness of the sample surfaces was first checked by the disappearance of a typical structure related to Cr oxides. We could also check the degree of contamination from the magnitude of the MCD signal, because its amplitude grew and finally saturated when the sample surface became clean enough. We considered that the unscraped or contaminated surface was covered with antiferromagnetic or paramagnetic compounds such as Cr oxides, which hardly contribute to the MCD spectrum. It is believed that the the total photoelectron yield from the scraped surfaces of the present samples reflect the absorption spectrum in the core-excitation region. The temperatures during the measurement were ~ 100 K for $CdCr_2Se_4$ and room temperature for $CuCr_2S_4$ and $CuCr_2Se_4$. This gives ~ 75, 60, and 80 % of the $T=0$ magnetization for $CdCr_2Se_4$, $CuCr_2S_4$, and $CuCr_2Se_4$, respectively.

III. BAND STRUCTURE AND MULTIPLET CALCULATIONS

Our relativistic band structure calculations were carried out by the linear muffin-tin orbital (LMTO) method[13,14] in the local spin density approximation by using scalar relativistic MT orbitals. The calculation includes spin-orbit coupling (SOC) in the variational procedure, which implies that the SOC Hamiltonian is diagonalized using the scalar relativistic wave functions as a basis set. Because of the weakness of SOC compared to the crystal field and exchange splittings in spinels under consideration, such a perturbative procedure is justified. Furthermore, since SOC contribution

TABLE I. *Ab initio* Hartree-Fock values of the Slater integrals and spin-orbit coupling constants (in units of eV). In the actual calculation, the Slater integrals have been scaled to 80% of these values to take into account intra-atomic relaxation effect.

	Configuration	$F^2(d,d)$	$F^4(d,d)$	$F^2(p,d)$	$G^1(p,d)$	$G^3(p,d)$	$\xi(2p)$	$\xi(3d)$
Cr^{4+}	d^2	11.794	7.437					0.041
	p^5d^3	12.573	7.928	7.210	5.396	3.071	5.668	0.053
Cr^{3+}	d^3	10.777	6.754					0.035
	p^5d^4	11.595	7.269	6.525	4.787	2.722	5.667	0.047

is of the first order (i.e., $\propto \xi$, the SOC parameter) and the SOC matrix elements between states with opposite spins are of the second order (i.e., $\propto \xi^2$), the latter can be omitted. In the iterations towards self-consistency of the single-particle effective crystal potential, both the exchange splitting and SOC were considered on an equal footing, i.e., both of these terms were effective in the formation of the crystal potential.

We have calculated the total and local orbital magnetic moments which are given by

$$l = \sum_{\sigma l m_l} m_l \cdot n_{m_l}^{\sigma},$$

where m_l is the magnetic quantum number corresponding to the orbital quantum number l and $n_{m_l}^{\sigma}$ is the occupied number density for spin σ.[15] Considering the calculated electronic structures, one should bear in mind that we have used the atomic-sphere approximation (ASA), and this implies that the choice of the sphere radii affects the amplitudes of the calculated magnetic moments.

In the analysis of the MCD of the Cr $2p$ XAS spectra, we have done full multiplet calculations based on the atomic model (with a single electronic configuration), neglecting charge transfer from surrounding orbitals. In this calculation, a crystal field in O_h symmetry ($10Dq$) has been applied. In order to induce a magnetic moment, a molecular field of 10 meV has been applied on the electron spin. Parameters for the intra-atomic electrostatic interactions are listed in Table I.

IV. RESULTS AND DISCUSSION

The XAS and MCD spectra in the Cr $2p$ core ($L_{2,3}$) excitation region of $CdCr_2Se_4$, $CuCr_2S_4$, and $CuCr_2Se_4$ are shown in Figs. 1(a) and 1(b). The XAS intensities I_+ and I_- have been normalized at a higher photon energy where no asymmetry is expected. The XAS spectrum for the Cr^{3+} compound $CdCr_2Se_4$ shows a white line at each spin-orbit component of the $2p$ core without any remarkable multiplet structure. A shoulder structure is located on the lower energy side of the $2p_{3/2}$ main peak. It is found that the energy position of the spectrum I_+ is lower than that of I_- for both of the $2p_{3/2}$ and $2p_{1/2}$ components, resulting in the positive-negative feature in the MCD ($I_+ - I_-$) spectra with increasing photon energy ($h\nu$) as shown in Fig. 1(b). The integrated MCD signal over the measured $h\nu$ range is negligibly small ($\langle L_z \rangle < 0.1\mu_B$), indicating almost quenched orbital moment contribution to the magnetic moment on the Cr atom in

$CdCr_2Se_4$. The XAS and MCD spectra of $CuCr_2S_4$ and $CuCr_2Se_4$ are almost identical to that of $CdCr_2Se_4$ except for the degree of the peak asymmetry. The orbital magnetic moment is almost quenched in the Cu-based compounds, too.

The line shapes of the XAS and MCD spectra are believed to be strongly dependent on the electronic states or the electronic configuration of the atom. To see further such changes of the line shapes of XAS and MCD spectra depending on the electronic states, we have carried out multiplet calculations for the Cr $2p$ XAS and MCD spectra assuming Cr $3d^3$ and $3d^2$ configurations for the ground state. Here, the mixing between the d^3 and d^2 configurations has not been taken into account. Before showing calculated spectra, it is useful to see the dependence of the magnetic moments on the crystal field. Figure 2 shows the calculated spin, orbital and total magnetic moments for the (a) d^3 and (b) d^2 configurations in the ground state as a function of the octahedral crystal field $10Dq$. Here, a positive $10Dq$ value corresponds to the octahedral (O_h symmetry) coordination, whereas a negative one is for the tetrahedral (T_d symmetry) coordination. For the d^3 configuration, one clearly finds comparable but antiparallel contribution of spin and orbital magnetic moments at zero crystal field. For a positive crystal field of $10Dq > 1$ eV, the orbital moment is almost quenched and the spin magnetic moment ($\approx$ total magnetic moment) becomes closer to $3\mu_B$. This is easily understood if the energy levels of the Cr^{3+} ion octahedrally surrounded by the S or Se atoms is considered. Here, the three $3d$ electrons occupy the threefold degenerate majority-spin t_{2g} orbitals, leading to the vanishing orbital moment as schematically drawn in Fig. 2(c). On the contrary, for the d^2 configuration, a larger orbital magnetic moment appears for a positive large crystal field as shown in Figs. 2(b) and 2(c). In the spinel type structure, the local coordination of the B site has the trigonal distortion along the $\langle 111 \rangle$ direction. In this case, the threefold degenerate t_{2g} level splits into two levels, such as a nondegenerate level (a_{1g}) and a twofold degenerate level (e_g). It is expected that the orbital moment is quenched even for the d^2 configuration in the case of the shortened structure along the $\langle 111 \rangle$ direction because the twofold degenerate e_g level is located below a_{1g} in energy.[16,17] On the contrary, the elongated structure as in the case of the spinel structure does not affect the orbital magnetic moment.

The calculated isotropic Cr $2p$ XAS spectra of the d^3 ground state configuration for $10Dq = 0$, 1, and 2 eV are shown in Fig. 3. The experimental isotropic spectrum obtained as $(I_+ + I_-)/2$ of $CuCr_2Se_4$ is also shown for com-
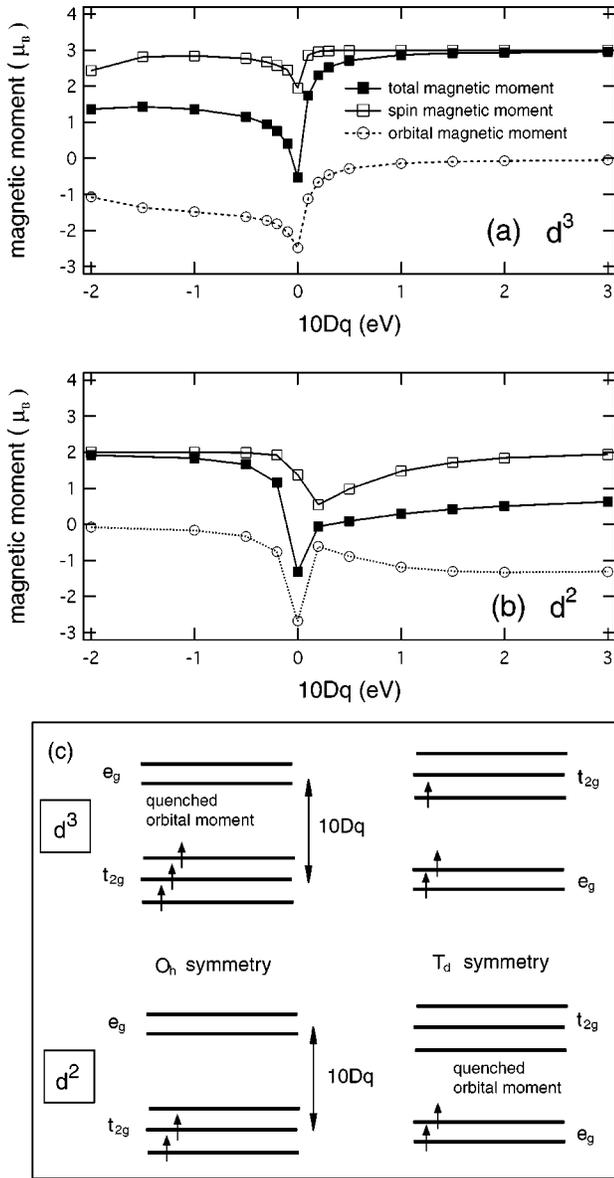
FIG. 2. Calculated spin (open square), orbital (open circle) and total (filled square) magnetic moments for the (a) d^3 and (b) d^2 configurations in the ground state as a function of octahedral crystal field $10Dq$. (c) Schematic representation of the symmetry dependence of the orbital moment for d^3 (upper) and d^2 (lower) configurations.

parison. It is noted that the spectral line shape of the calculated spectrum with $10Dq=0$ eV is much different from that of the experimental spectrum. Especially, there exists a sharp structure in the calculated spectrum in the intermediate region between $2p_{3/2}$ and $2p_{1/2}$ components, which is not observed in the experimental spectrum. One can find some correspondences in the energy positions of the structures between the experimental spectrum and the calculated one with $10Dq=2.0$ eV for the structures denoted by A–E. Figure 4 shows the calculated Cr $2p$ MCD spectra of the d^3 ground state configuration for $10Dq=0$, 1, and 2 eV. The calculated MCD feature at $10Dq=0$ eV shows positive-negative signal with increasing photon energy in the $2p_{3/2}$ region,
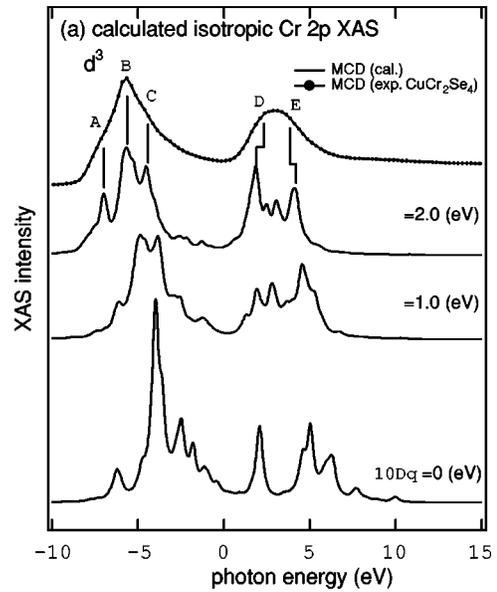
FIG. 3. Calculated isotropic XAS spectra obtained as $(I_+ + I_-)/2$ in the Cr $2p$ core (L_{23}) excitation region of the d^3 ground state configuration for $10Dq=0$, 1, and 2 eV. The experimental MCD spectrum of CuCr$_2$Se$_4$ is also shown for comparison.

whereas only minus signal appears in the $2p_{1/2}$ region. In the experimental MCD spectrum, such a positive-negative structure is observed not only in the $2p_{3/2}$ region but also in the $2p_{1/2}$ region, which is not reproduced in the calculated spectrum for the zero crystal field. For a finite crystal field of 1.0 eV, for example, a positive-negative structure appears in the $2p_{1/2}$ region as well as in the $2p_{3/2}$ region. One finally finds some correspondence between the observed Cr $2p$ MCD spectrum and the calculated ones for $10Dq=2.0$ eV. It is noticed that the small-positive feature indicated by F as well as the large positive structure (G) is reproduced in the calculated multiplets for $10Dq=2.0$ eV except for the small energy shifts of the positive (H) and negative (I) signals in the $2p_{1/2}$ region. On the other hand, the line shapes of the calculated spectra for the d^2 ground state configuration are much different from those for the d^3 configuration. For the d^2 configuration, one notices that the positive-negative feature does not appear both in the $2p_{3/2}$ and $2p_{1/2}$ components. It is considered that the experimental Cr $2p$ MCD spectra of CdCr$_2$Se$_4$, CuCr$_2$S$_4$, and CuCr$_2$Se$_4$ are well explained by the calculated multiplets of the d^3 configuration and the crystal field of 2 eV in the $O_{\rm h}$ symmetry. The similarity of the spectra between the Cd-based and Cu-based compounds implies that the valency of the Cr atoms in the Cu-based Cr spinels is nearly 3+ in spite of the formal valence of Cr$^{3.5+}$ and that the Cr atom has negligibly small orbital moment. The additional holes in the Cu-based compounds probably go into the S $3p$ /Se $4p$ bands and not in the Cr $3d$ bands. The early transition metal (Sc-Cr) compounds was originally classified in the Mott-Hubbard regime ($U<\Delta$), where U is the on-site $d-d$ Coulomb repulsion energy and Δ is the charge transfer energy.[18] Recent configuration-interaction cluster-calculation analyses of core-level photoemission
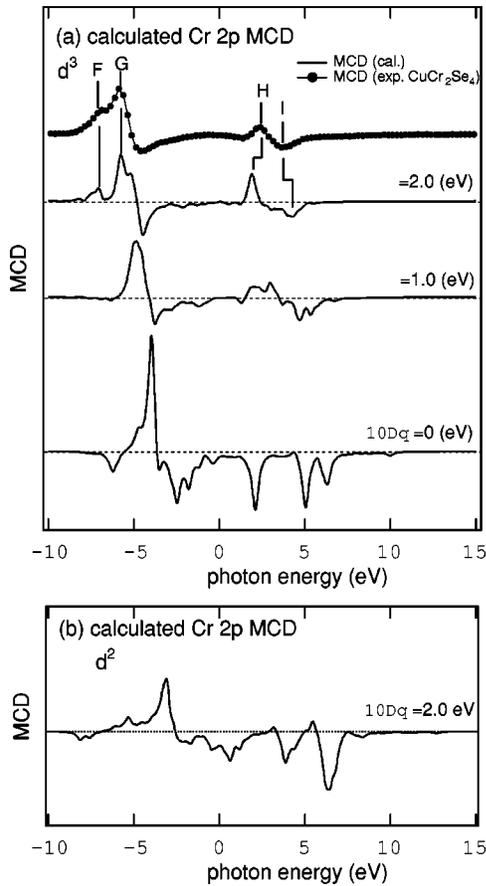
FIG. 4. Calculated MCD ($I_+ - I_-$) spectra in the Cr $2p$ core (L_{23}) excitation region of the d^3 ground state configuration for $10Dq = 0$, 1 and 2 eV (a) and the d^2 ground state configuration for $10Dq = 2$ eV (b). The experimental MCD spectrum of $CuCr_2Se_4$ is also shown for comparison.

spectra have shown that the Cr oxides such as Cr_2O_3 and $LaCrO_3$ are classified in the intermediate region between the Mott-Hubbard and charge-transfer regimes ($U \simeq \Delta$).[19] It is, therefore, considered that Cr sulfides and selenides can be classified in the charge-transfer regime ($U > \Delta$) due to the smaller electron negativities of S or Se compared to oxygen. This is consistent with the above mentioned picture that the additional holes go into the S $3p$ /Se $4p$ bands of $CuCr_2S_4$ and $CuCr_2Se_4$.

Figures 5(a) and 5(b) show the XAS and MCD spectra of $CuCr_2S_4$ and $CuCr_2Se_4$ in the Cu $2p$ core ($L_{2,3}$) excitation region. The Cu $2p$ XAS spectra for these Cu-based compounds show a double-peak structure separated by ~ 6 eV for $CuCr_2S_4$ and 6.6 eV for $CuCr_2Se_4$ in each region of the $2p_{3/2}$ and $2p_{1/2}$ components. It is noticed that clear MCD appears at the first peak of each component, whereas MCD signal is completely absent for the second peak of the same component. Nonzero asymmetry as observed in the pre edge region of Cu $2p$ XAS spectrum of $CuCr_2S_4$ [Fig. 5(a)] is considered to be caused by our experimental error. The appearance of the MCD signals for these Cu-based Cr chalcogenides shows induced magnetic moment on the Cu site. One can notice that the polarity of the MCD signal for the
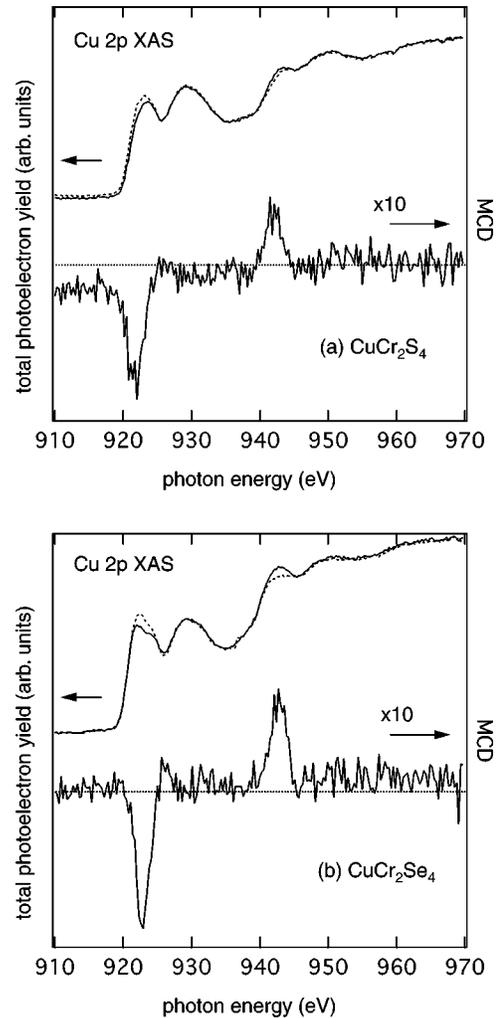
FIG. 5. Experimental Cu $2p$ XAS (upper) and MCD (lower) spectra of (a) $CuCr_2S_4$ and (b) $CuCr_2Se_4$. I_+ (I_-) is indicated by solid (dashed) line.

Cu $2p$ absorption spectrum is oppsite to that of the Cr $2p$ spectra. This shows antiparallel alignment of the magnetic moments between the Cu $3d$ and Cr $3d$ states. From these results, the first peak can be assigned to transitions from the Cu $2p$ core to the Cu $3d$ states which are well hybridized with the Cr $3d$ states and the second peak to transitions to the empty Cu $4s$ states, which may be hybridized primarily with the anion (S or Se) $4p$ state.

In order to interpret the above results, we have performed band-structure calculations using the relativistic LMTO method for $CdCr_2Se_4$, $CuCr_2S_4$, and $CuCr_2Se_4$. The spin and orbital magnetic moments per atom for the Cd, Cu, Cr, S, and Se atoms have been calculated as shown in Table II. The right three columns show the calculated total spin (M_s), orbital (M_l), and the measured total magnetic moments ($M_s + M_l$) per formula unit MCr_2X_4 ($M = Cd$, Cu: $X = S$, Se). The theoretical net magnetic moments ($M_s + M_l$) per formula unit are $5.977\mu_B$ for $CdCr_2Se_4$ and $4.950\mu_B$ for $CuCr_2S_4$ and $5.032\mu_B$ for $CuCr_2Se_4$, which are in reasonable agreement with the experimental values obtained by the

TABLE II. Calculated spin (m_s) and orbital (m_l) magnetic moments by the relativistic LMTO method for Cd, Cu, Cr, S, and Se atoms in the spinel Cr chalcogenides (in units of μ_B). The experimental site projected magnetic moments per atom from the present MCD results and the neutron diffraction experiments are also listed for comparison. The right three columns show the total spin (M_s), orbital (M_l) and the measured total magnetic moments ($M_s + M_l$) per formula unit MCr_2X_4 (M=Cd, Cu: X=S, Se).

Compound	Atom	m_s	m_l	expt. ($m_s + m_l$)	M_s	M_l	expt. ($M_s + M_l$)
	Cd	−0.004	0.0				
$CdCr_2Se_4$	Cr	3.193	−0.006	2.93 [a]	6.00	−0.023	5.98 [d]
	Se	−0.103	−0.003				
	Cu	−0.078	−0.005	−0.07±0.02 [b]			
$CuCr_2S_4$	Cr	2.704	−0.030	2.93, [a] 2.64±0.04 [b]	5.017	−0.067	
	S	−0.104	−0.001	−0.05±0.11 [b]			
	Cu	−0.086	−0.014	0.01±0.13, [c] −0.1 [b]			
$CuCr_2Se_4$	Cr	2.866	−0.014	2.93, [a] 2.81±0.11 [c]	5.100	−0.068	5.07 [e]
	Se	−0.149	−0.007	−0.25±0.14 [c]			5.03±0.13 [f]

[a]Present MCD experiment.
[b]Reference 23.
[c]Reference 24: neutron diffraction measurement.
[d]Reference 20.
[e]Reference 22.
[f]Reference 21: magnetization measurement. [The evaluated magnetic moment ($m_s + m_l$) on the Cr site from the present MCD experiment is $2.93\mu_B$ per Cr atom. This is decomposed into the spin magnetic moment (m_s) of $3\mu_B$ and the orbital magnetic moment (m_l) of $-0.07\mu_B$.]

magnetization measurements of $5.98\mu_B$ (Ref. 20) and $5.03 \pm 0.13\mu_B$ (4.2 K) (Ref. 21) for $CdCr_2Se_4$ and $CuCr_2Se_4$, respectively. The experimentally obtained site-projected magnetic moments ($m_s + m_l$) per Cr atom by a neutron diffraction study in $CuCr_2S_4$ and $CuCr_2Se_4$ are $2.64\pm0.04\mu_B$ (Ref. 23) and $2.81\pm0.11\mu_B$,[24] which are consistent with our theoretical values ($m_s + m_l$) of $2.674\mu_B$ and $2.852\mu_B$, respectively. In this way, the theoretical total magnetic moment and the site projected magnetic moment for the Cr atom by the band structure calculation are reproduced well. Interestingly, the spin magnetic moments of the Cu site in $CuCr_2S_4$ and $CuCr_2Se_4$ are as large as -0.078 and $-0.086\mu_B$ per Cu atom, respectively, which are antiparallel to that of the Cr site, consistent with the present MCD result. A determination of the magnetic moment using sum rules[9,10] for lighter transition metal elements such as Cr is questionable especially for the spin magnetic moment because the $2p_{3/2}$ and $2p_{1/2}$ edges are not well separated and are mixed with each other.[25] In this case, the best way to derive the magnetic moments is to fit the calculated spectrum to the experimental one using the multiplet calculation as already discussed above (Figs. 3 and 4). In this way, we have obtained the spin and orbital magnetic moments of $3\mu_B$ and $-0.07\mu_B$, respectively and the total magnetic moment ($m_s + m_l$) of $2.93\mu_B$ as listed in Table II, which are consistent with the values obtained by our LMTO band structure calculations and the neutron diffraction measurements.[23,24] Although the absolute values of the magnetic moments are difficult to be obtained from the sum rule, the ratio between the moments of the Cr and Cu sites can be discussed. The MCD at the peak of the Cr $2p_{3/2}$ edge is estimated to be 6.70%. In the case of Cu $2p_{3/2}$ edge, the evaluated MCD is 10 times smaller (0.66%) than that of the Cr $2p_{3/2}$ edge indicating that the spin magnetic moment on the Cu site is expected to be roughly more than 10 times smaller than that of the Cr. The ratios of the calculated spin magnetic moment of the Cu site to that of the Cr site are -0.03 for the sulfide and selenide. In this way, the LMTO calculation explains well our experimental MCD result.

V. CONCLUSION

We have performed a soft x-ray absorption spectroscopy for several Cr spinel chalcogenides. The Cr $2p$ core excited XAS and MCD spectral features of the metallic ferromagnets $CuCr_2S_4$ and $CuCr_2Se_4$ are similar to that of the semiconducting $CdCr_2Se_4$. This means that the net d-electron numbers of Cr are not much different between the Cu based and Cd based compounds in spite of the different formal valencies of Cr, $Cr^{3.5+}$, and Cr^{3+}, respectively. We have also found that the magnetic moment of the Cu $3d$ state of the Cu-based Cr spinels remains finite and is aligned antiparallel to that of Cr. This result is well explained by the relativistic band-structure calculations. The present experimental MCD and the calculated results partially support the Goodenough's assumption that the octahedral sites are occupied by the Cr^{3+} ions. However, our result shows that the tetrahedral sites are occupied not by divalent Cu ions but by nearly monovalent ions, with a small amount of holes inducing the small magnetic moment, which is contrary to Goodenough's interpretation.[1] It is then proposed that the extra holes in the Cu-based compounds goes to the Se $4p$/S $3p$ band. This proposal is reasonable because the spinel type Cr sulfides

and selenides can be classified in the charge transfer type materials.

---

*Electronic address: akimura@hisor.material.sci.hiroshima-u.ac.jp Present address: Department of Physical Sciences, Graduate School of Science, Hiroshima University, Kagamiyama 1-3-1, Higashi Hiroshima 739-8526, Japan.

[1] J. B. Goodenough, J. Phys. Chem. Solids **30**, 261 (1969).

[2] K. Dwight and N. Menyuk, Phys. Rev. **163**, 435 (1967).

[3] T. Kambara, T. Oguchi, and K. Gondaira, J. Phys. C **13**, 1493 (1980).

[4] T. Oguchi, T. Kambara, and K. I. Gondaira, Phys. Rev. B **22**, 872 (1980).

[5] W. J. Miniscalco, B. C. McCollum, N. G. Stoffel, and G. Margaritondo, Phys. Rev. B **25**, 2947 (1982).

[6] M. Taniguchi, A. Fujimori, and S. Suga, Solid State Commun. **70**, 191 (1989).

[7] F. K. Lotgering and R. P. van Stapele, Solid State Commun. **5**, 143 (1967).

[8] A. P. Ramirez, R. J. Cava, and J. Krajewski, Nature (London) **386**, 156 (1997).

[9] B. T. Thole, P. Carra, F. Sette, and G. van der Laan, Phys. Rev. Lett. **68**, 1943 (1992).

[10] P. Carra, B. T. Thole, M. Altarelli, and X. Wang, Phys. Rev. Lett. **70**, 694 (1993).

[11] Y. Kagoshima, T. Miyahara, S. Yamamoto, H. Kitamura, S. Muto, S.-Y. Park, and J.-D. Wang, Rev. Sci. Instrum. **66**, 1696 (1995).

[12] S. Muto, Y. Kagoshima, and T. Miyahara, Rev. Sci. Instrum. **63**, 1470 (1992).

[13] O. K. Andersen, Phys. Rev. B **12**, 3060 (1975).

[14] Yu. A. Uspenskii, E. T. Kulatov, and S. V. Halilov, Phys. Rev. B **54**, 474 (1996).

[15] M. S. S. Brooks and P. J. Kelly, Phys. Rev. Lett. **51**, 1708 (1983).

[16] S. Sugano, Y. Tanabe, and H. Kamimura, *Multiplets of Transition-Metal Ions in Crystals* (Academic Press, New York, 1970).

[17] G. van der Laan and B. T. Thole, Phys. Rev. B **43**, 13 401 (1991).

[18] J. Zaanen, G. A. Sawatzky, and J. W. Allen, Phys. Rev. Lett. **55**, 418 (1985).

[19] A. E. Bocquet, T. Mizokawa, K. Morikawa, A. Fujimori, S. R. Barman, K. Maiti, D. D. Sarma, Y. Tokura, and M. Onoda, Phys. Rev. B **53**, 1161 (1996).

[20] R. C. LeCraw, H. von Philipsborn, and M. D. Sturge, J. Appl. Phys. **38**, 965 (1967).

[21] H. Brändle, J. Schoenes, P. Wachter, F. Hulliger, and W. Reim, Appl. Phys. Lett. **56**, 2602 (1990).

[22] I. Nakatani, H. Nose, and K. Masumoto, J. Phys. Chem. Solids **39**, 743 (1978).

[23] O. Yamashita, Y. Yamaguchi, I. Nakatani, H. Watanabe, and K. Masumoto, J. Phys. Soc. Jpn. **46**, 1146 (1979).

[24] C. Colominas, Phys. Rev. **153**, 558 (1967).

[25] Y. Teramura, A. Tanaka, and T. Jo, J. Phys. Soc. Jpn. **65**, 1053 (1996).